

Available online at www.sciencedirect.com

ScienceDirect

journal homepage: www.jfda-online.com

Original Article

Novel electrochemical xanthine biosensor based on chitosan–polypyrrole–gold nanoparticles hybrid bio-nanocomposite platform



Muamer Dervisevic^{a,*}, Esmā Dervisevic^a, Emre Çevik^b, Mehmet Şenel^{b,*}

^a Mehmed-pase-Sokolovica, No 21, Bihac 77000, Bosnia and Herzegovina

^b Biotechnology Research Lab, EMC Technology Inc, ARGEM Building, Technocity, Avclar, Istanbul 34320, Turkey

ARTICLE INFO

Article history:

Received 29 June 2016

Received in revised form

28 November 2016

Accepted 25 December 2016

Available online 15 February 2017

Keywords:

amperometric biosensor

bio-nanocomposite

chitosan

gold nanoparticles

xanthine oxidase

ABSTRACT

The aim of this study was the electrochemical detection of the adenosine-3-phosphate degradation product, xanthine, using a new xanthine biosensor based on a hybrid bio-nanocomposite platform which has been successfully employed in the evaluation of meat freshness. In the design of the amperometric xanthine biosensor, chitosan–polypyrrole–gold nanoparticles fabricated by an *in situ* chemical synthesis method on a glassy carbon electrode surface was used to enhance electron transfer and to provide good enzyme affinity. Electrochemical studies were carried out by the modified electrode with immobilized xanthine oxidase on it, after which the biosensor was tested to ascertain the optimization parameters. The Biosensor exhibited a very good linear range of 1–200 μM , low detection limit of 0.25 μM , average response time of 8 seconds, and was not prone to significant interference from uric acid, ascorbic acid, glucose, and sodium benzoate. The resulting bio-nanocomposite xanthine biosensor was tested with fish, beef, and chicken real-sample measurements.

Copyright © 2017, Food and Drug Administration, Taiwan. Published by Elsevier Taiwan LLC. This is an open access article under the CC BY-NC-ND license (<http://creativecommons.org/licenses/by-nc-nd/4.0/>).

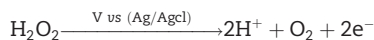
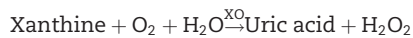
1. Introduction

Xanthine is a purine base derived from guanine and adenosine-3-phosphate (ATP) [1] catabolism in the muscle tissues of animals, and accumulation usually results in death. Xanthine metabolism is a sequence where ATP is hydrolyzed to give adenosine, followed by sequential conversion into inosine monophosphate, inosine, hypoxanthine, xanthine, uric acid (UA), and finally urate, by means of enzyme action. Abnormal

xanthine levels in human plasma and urine may contribute to deregulation of xanthine metabolism, and an excess amount of xanthine acquired through spoiled food with an unpleasant smell could eventually lead to physiological problems such as gout [2], xanthinuria [3], hyperuricemia [4], and preeclampsia [5]. As well as being a biomarker for the stated diseases, xanthine is also an indicator for fish and meat spoilage and freshness determination [6]. Xanthine oxidase (XO) is widely distributed in mammalian tissue and it is a key enzyme in

* Corresponding authors. Biotechnology Research Lab, EMC Technology Inc, ARGEM Building, Technocity, Avclar, Istanbul 34320, Turkey
E-mail addresses: muamerdervisevic@gmail.com (M. Dervisevic), msenel81@gmail.com (M. Şenel).
<http://dx.doi.org/10.1016/j.jfda.2016.12.005>

purine metabolism [7] which makes it an ideal biomolecule candidate for the design of amperometric biosensors. Amperometric detection of xanthine requires no complex sample preparation and provides fast analysis with lower cost [7] through the electrochemical reaction indicated with the basic working principle [8]:



$2\text{e}^- \rightarrow$ Working electrode

Amperometric xanthine biosensors as an electrochemical method easily overcomes contemporary necessities in xanthine detection when compared with other traditional methods such as: (1) capillary column gas chromatography [9]; (2) enzymatic colorimetric method [10]; (3) high pressure liquid chromatography [11]; (4) enzymatic fluorometric method [12]; and (5) fluorometric mass spectrometry fragmentography [12], which have the disadvantages of taking a long time for sample preparation, requiring skilled personnel to operate highly specialized equipment, the impossibility of onsite detection, complex sample pretreatment, etc. Conversely, amperometric biosensing is a straightforward method which takes a short time for analysis, has no need for highly skilled personal, and most importantly there is no need for sample pretreatment and it is suitable for onsite detection. XO is an important part of the amperometric xanthine biosensor but its full efficiency is observed when applied with a proper immobilization matrix or conducting polymers. Due to flexibilities provided by the conducting polymers in chemical structure modifications, they have offered a great deal for novel applications in various fields [13], where, among different conducting polymers, polypyrrole (PPy) has particularly attracted attention [14]. Efficient electron transfer ability, manageable and homogeneous film character, reproducibility and easy production, availability of various types of monomers, stability and biocompatibility, and ability to modify physical and optical properties are some of many reasons for the use of conducting polymers in biosensor design [15].

Chitosan [(1→4)-2-amino-2-deoxy-d-glucan] is a natural polysaccharide derived by the deacetylation of natural chitin [16] and it received much attention in biological field applications because of its linear and hydrophilic properties. As well as its attractive biocompatibility and excellent film-forming ability which is a result of its biodegradable and nontoxic nature, chitosan can be used as a modification agent thanks to its hydroxyl and amino functional groups which can react with bioactive molecules [17] and as such is used as a substrate for the covalent immobilization of enzymes. Chitosan-based biosensors are facing problems related to the transfer of the electric signal to the transducer, due to the relatively low conductivity of chitosan [17]. To improve the conductive properties of chitosan, materials such as carbon nanotubes, ferrocene, thiourea, ethylene diamine, urocanic acid [18], and nanoparticles (NPs) were combined with chitosan in order to make nanocomposites.

Nanocomposites containing the conducting polymer, biopolymer, and metal NPs have received considerable

attention due to their wide range of applications, such as electro-catalysis, chemical sensors, and microelectronic devices [19,20]. These kinds of nanocomposite layers are also good candidates for the formation of a biosensing layer by immobilization of biorecognition molecules [21,22]. Compared with nanocomposites constructed by insulating polymers, conducting polymers can serve as a novel electroactive relay among metal NPs in the nanocomposite matrix [23]. Therefore, the fabrication of novel nanocomposites based on metal NPs and conducting polymers would provide various beneficial characteristics and new features in nanotechnological applications.

Among all metal NPs, gold NPs have been widely used due to their unique properties such as catalytic activities, optical properties, and biocompatibility. Applications have been reported where gold NPs were dispersed onto different materials such as carbon paste electrode, self-assembled monolayer, and conducting and nonconducting polymers, to obtain a biosensor interface [24]. The composite of polymer and gold NPs, various monomers, and polymers could be chosen. Because the stabilization of gold NPs with chitosan has been extensively studied [25], the method chosen for the present work is gold NPs prepared through a simple chemical reduction process, using pyrrole monomer to construct a biosensor by means of a simple one-step process on the chitosan-modified electrode surface [26].

In this study we report first an amperometric xanthine biosensor based on hybrid bio-nanocomposite platform designed for measuring xanthine, which can easily compete with most of the xanthine biosensors reported. The biosensor is fabricated by *in situ* chemical synthesis on a glassy carbon electrode (GCE) surface using chitosan–PPy–gold (Chi–PPy–Au) NPs and with subsequent immobilization of XO. The resulting biosensor showed very good analytical performance, as well as excellent real-sample application. The reliability of the fabricated electrode was tested with fish, beef, and chicken samples in different time intervals (days) and demonstrated easy, fast, reliable, and accurate measurements of xanthine and would therefore give precise results in meat quality control.

2. Methods

2.1. Materials

XO, xanthine, 1-ethyl-3-(3-dimethylaminopropyl)carbodiimide hydrochloride (EDC) and 1-(2-cyanoethyl)pyrrole (Py-CN) were purchased from Sigma-Aldrich, Germany. Hydrogen tetrachloroaurate(III) hydrate (HAuCl₄) 99.9% (metals basis) and Au (minimum 49%) were purchased from Alfa Aesar, USA, and pyrrole was purchased from Merck, Germany. All other chemicals were of analytical grade and were used without further purification.

2.2. Synthesis of pyrrole-branched chitosan

1-(2-carboxyethyl) pyrrole (PyPA) was obtained by hydrolysis of Py-CN according to the literature [27]: a mixture of 25 g of Py-CN and 100 mL of 15% potassium hydroxide solution was

stirred at 50°C for 40 h. The mixture was then cooled to room temperature and acidified using hydrochloric acid. After extraction with ether, the crude product (colorless crystals) was collected on evaporation of ether. The product was dissolved in ether and purified by recrystallization from the ether solution. The product was identified as PyPA by means of FTIR-ATR, ¹H, and ¹³C NMR spectroscopy (not shown).

EDC coupling reaction was used to synthesize pyrrole-branched chitosan through amide bonds formation. Methanol was added to 1% (w/v) chitosan dissolved in acetic acid solution in order to obtain 85:100 mL methanol and chitosan solution, respectively. The addition of PyPA to the chitosan solution in the ratio of 0.54 mol/mol glucosamine residue of chitosan was followed by adding 15 mL of 0.07% (w/v) EDC dissolved in methanol when stirred at room temperature. In the current study, equal moles of EDC and PyPA were used. At the end of 24 hours, the reaction mixture was transferred into 200 mL of 7/3 (v/v) methanol/ammonia solution while being stirred. The primitive product was then filtered and washed with distilled water (DW), methanol, and ether, respectively, followed by drying under vacuum for 24 hours at room temperature. This procedure was followed and performed as reported by Liu et al [28].

2.3. Preparation of enzyme electrode

Prior to modifications, a GCE was polished with 0.3 μm alumina slurry diluted with DW on a microcloth pad, washed with distilled water DW and acetone, respectively, and left to air-dry at room temperature. The electrode surface was covered using a drop-coating method with chitosan–pyrrole (Chi–Py), pyrrole, and 1% HAuCl₄ (5:1:1) being dripped separately and observing the Au-NP formation from the occurrence of a dark reddish-brown color. After drying the electrode at room temperature, the coating procedure was prolonged by immersing in 2% glutaraldehyde, then in 9 mg/mL of XO, and left to dry at 4°C for 1.5 hours. The solutions dripped onto the electrode surface were uniformly distributed. The working electrode was kept at 4°C in phosphate buffered saline (PBS; 10 mM, pH 7.0) while not being used.

2.4. Xanthine determination in meat samples

In order to investigate xanthine concentration as a meat-spoilage marker, samples of chicken, fish, and beef were purchased from the local market and left for 5 days, 10 days, 15 days, 20 days, and 25 days at room temperature so that the spoilage process could occur. The samples were then cut into pieces, homogenized, and mixed with DW at a ratio of 1:5 (w/w), respectively. Afterwards, the homogenate was filtered with filter paper and the content of xanthine was determined using the described biosensor under optimal conditions. The reason for testing the fabricated electrode using fresh samples stored at room temperature was to evaluate the efficiency of the electrode in detection of xanthine at different stages of meat spoilage. Data were interpolated using a standard curve (concentration vs. current) prepared under optimal working conditions of the biosensing electrode.

2.5. Instrumentation

Electrochemical measurements were performed using CompactSoft portable electrochemical interface and impedance analyzer (Ivium Technologies, Netherlands). The electrochemical measurements were recorded via a three-electrode system set at a working potential of + 0.70 V, composed of Ag/AgCl as reference, platinum wire as auxiliary, and Chitosan–PPy–Au-NPs as a working electrode, all immersed in an electrochemical cell filled with 10 mM PBS (pH 7.0). A conventional three-electrode electrochemical cell was purchased from CH Instruments, USA. After allowing the steady-state current to be reached, the xanthine catalysis was triggered by xanthine additions to the buffer solution by continuously stirring the working cell at room temperature. The substrate solution was freshly prepared by dissolving xanthine in 3:7 (v/v) 0.1 M NaOH and PBS, respectively, and the amperometric responses were recorded with the addition of known amounts of xanthine solution. Electrochemical impedance spectroscopy measurements were carried out using a CHI Model 6005 electrochemical analyzer in a background solution of 5 mM Fe³⁺/Fe²⁺ phosphate buffer (pH 7.0) at a normal potential. The alternating voltage was 5 mV and the frequency range was from 5.0 × 10⁻² Hz to 1.0 × 10⁶ Hz.

2.6. Analytical and statistical analysis of data

Each measurement was repeated five times and the standard deviation was calculated using the square root of variance formula:

$$S^2 = \frac{\sum (x - M)^2}{(N - 1)} \quad (1)$$

where M is the mean of the sample and N is the number of measurements (N = 5), and it was included in graphical representations as an error bar. Sensitivity was the biosensor's vital performance parameter, defined as slope of the calibration curve [29]:

$$S = d(\text{signal})/d(\text{concentration}) \quad (2)$$

where S is the sensitivity.

This equation is used in the linear range of the biosensor, in which the biosensor's signal is proportional to a change in concentration (Table 1). The limit detection is the smallest amount of analyte detectable by the biosensing electrode relative to the amount of analyte analyzed and it is determined by:

$$\text{LOD} = \frac{\text{std}}{S} \quad (3)$$

where LOD is the limit of detection, std stands for standard deviation of background signal, and S is sensitivity [29] (Table 1).

3. Results and discussion

3.1. Characterizations

Electrochemical characterizations of bare GCE, GCE/Chi–Py, and GCE/Chi–Py/Au nanocomposite coated electrodes were

Table 1 – Comparison of analytical performance of reported xanthine-based biosensors.

Electrode	LR (μM)	DL (μM)	RT (s)	Refs
PPy–XOD–Fe(CN) $_6^{4-}$	0–50 and 50–130	6.0	NR	[48]
XOD–GCPE	20–80	5.3	NR	[49]
XO/ZnO–NPs–PPy/Pt	0.8–40	0.8	5	[34]
Polyvinylchloride(PVC)/XO	0.025–0.4	0.025	30	[50]
XO/Co $_3$ O $_4$ /MWCNT/CS/GCE	0.2–16	0.2	5	[33]
CD–Au–NPs/XO–ADA	310–6.8 mM	150	14	[51]
P(GMA-co-VFc)/REGO-Fe $_3$ O $_4$	2–36	0.17	3	[52]
PPy–Fc/XO	5–20	NR	NR	[53]
XOx/Nano Fe $_3$ O $_4$ /Au	0.4–2.4 nM	2.5pM	2	[54]
XOD/c–MWCNT/PANI/Pt	0.6–58	0.6	5	[55]
Modified graphite/gelatin	0–40	4.5	120	[56]
Chitosan/PPy/Au–NPs	1–200	0.25	8	This work

DL = detection limit; LR = linear range; NR = not reported; RT = response time.

carried out by cyclic voltammetry (CV), as shown in Figure 1A. CVs were performed in 5 mM Fe^{II}(CN) $_6^{4-}$ /Fe^{III}(CN) $_6^{3-}$ as a model reversible redox couple at a potential range of –0.2 V to 0.7 V versus Ag/AgCl at a scan rate of 100 mV/s. As shown in Figure 1A, the response of the redox couple at the GCE/

Chi–Py/Au (Curve c) is much stronger than that at GCE/Chi–Py (Curve b). This enhanced electrochemical behavior is attributed to the presence of gold NPs in the polymeric film [30]. For further characterization, cyclic voltammograms of bare GCE, GCE/Chi–Py, and GCE/Chi–Py/Au electrodes in

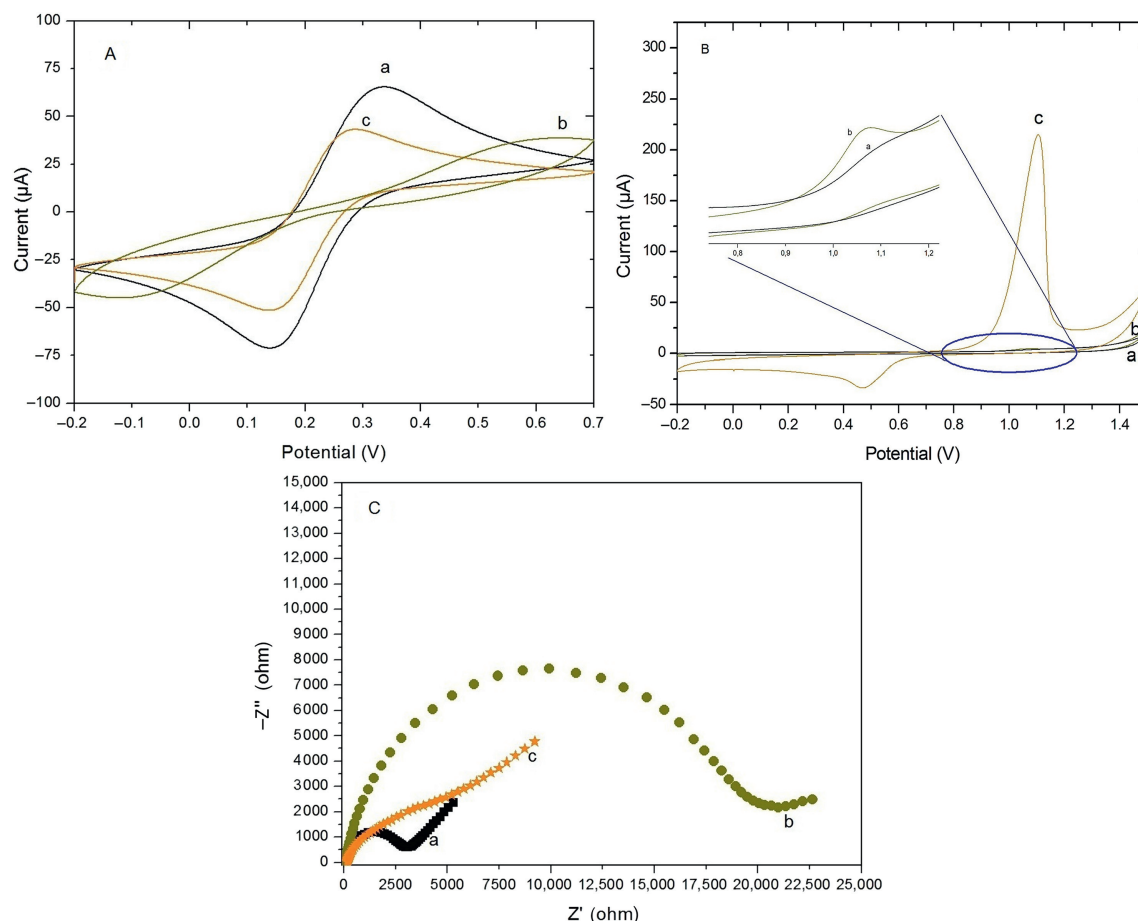


Figure 1 – (A) Cyclic voltammograms of (a) bare GCE, (b) GCE/Chi–Py, and (c) GCE/Chi–Py/Au electrodes in 10 mM PBS solution, pH 7.0 containing [Fe(CN) $_6$] $^{3-/4-}$ (5 mM). (B) Cyclic voltammograms of (a) bare GCE, (b) GCE/Chi–Py, and (c) GCE/Chi–Py/Au electrodes in 10 mM PBS solution, pH 7.0. (C) Electrochemical impedance spectra of (a) bare GCE, (b) GCE/Chi–Py, and (c) GCE/Chi–Py/Au electrodes in 10 mM PBS solution, pH 7.0 containing [Fe(CN) $_6$] $^{3-/4-}$ (5 mM). Chi = chitosan; GCE = glassy carbon electrode; Py = pyrrole.

100 mM PBS solution, pH 7.5, were performed (Figure 1B). An oxidation peak at 1.12 V was shown for the GCE/Chi-Py/Au electrode and attributed to the oxidation of Au⁰ to Au³⁺ in the form of Au₂O₃ [30]. An oxidation peak at 1.12 V of cyclic voltammogram confirms the presence of gold NPs in the Chi-Py film exist on the surface of the electrode. Also, the inset of Figure 1B shows the part of the cyclic voltammograms of the bare GCE and Chi-Py coated GCE. The current begins to increase at around 0.9 V, and then increases continuously with increasing potential, which is the indication of the formation PPy intra- or inter-polymer side chain. This peak cannot be observed easily in the voltammogram of the GCE/Chi-Py/Au electrode due to the huge peak of Au in the polymer composite film. Figure S1 demonstrates the performance of the biosensing electrode, which is determined based on the diffusion efficiency of the substrate and product at the surface layer of the electrode. The mass transfer efficiency of the electrode was studied by recording CV of Chi-PPy/Au-Xo electrode in the presence of 10 μM xanthine and H₂O₂. The results illustrate that mass transfer behavior of the fabricated electrode depends on H₂O₂ concentration. The immobilized enzyme on the polymer film had a very small effect on mass transfer when comparison is made between xanthine and H₂O₂ additions, demonstrating excellent performance of the biosensing electrode.

Electrochemical impedance spectroscopy would provide detailed information on changes of the surface electron transfer property of modified electrodes for each modification process. The typical impedance spectrum (represented in the form of the Nyquist plot) includes a semicircle portion at higher frequencies corresponding to the electron-transfer-limited process and a linear part at lower frequency range representing the diffusion-limited process. The semicircle diameter in the impedance spectrum is equal to the electron-transfer resistance, R_{et} , which reflects the electron-transfer kinetics of the redox probe at the electrode surface [31]. Figure 1C shows that the electron transfer resistance decreases in the order of the modified electrodes: bare GCE < GCE/Chi-Py/Au < GCE/Chi-Py, which indicates that the Au-NPs improve the conductivity of the composite film-modified GCE. The bare GCE exhibits small resistivity in the Nyquist plot; however, after coating the Chi-Py polymer film the value of R_{et} increases to 20,000 Ω. With the formation of Au-NPs in the chitosan polymer film with pyrrole cross linking, the R_{et} of the resultant Chi-Py/Au film drastically decreases, demonstrating that Au-NPs act as high electron relay for shuttling electrons between the electrochemical probe and the electrode. This was similarly reported by Lin et al [32] in a study showing that electrochemical impedance shows that gold NPs doped in chitosan decrease the resistance of chitosan-coated electrodes.

3.2. Determination of experimental variables

The applied potential effect on current response of the working electrode was investigated over the range of 0.40–0.80 V, as given in Figure 2A. The amperometric current of xanthine increased as potential increased from 0.40 V to 0.70 V, and then started to decrease with further potential increments. Therefore a potential of 0.70 V has been selected

as the optimum working potential for the biosensor and it was used in further experiments.

pH dependence of the enzyme electrode was investigated over a range of pH 4.0–8.0 in 10 mM PBS in the presence of xanthine. The optimum amperometric response was obtained at pH 7.0 (Figure 2B), which indicates that the immobilization technique has no big influence on the optimum pH of XO, as reported in the literature [33,34]. As seen in Figure 2B, when pH is ≤ 4.0, the biosensor showed 4% of total response, indicating deactivation of the enzyme. These results may occur because the acidic medium causes enzyme deformations and leads to loss of catalytic capability [35]. Amperometric response increases with pH increments until it reaches the maximum response at pH 7.0, where further increments resulted in the gradual decrement of amperometric response. Therefore, pH 7 was selected as the working pH of PBS in further experiments.

The effect of temperature on the electrochemical response of the electrode was studied across a range of 25–45°C. The response current of the Chi-PPy/Au-NPs/XO electrode progressively increased from 25°C to 40°C, after which the response drastically decreased at higher temperatures (Figure 2C). It was also observed that heat resistance of XO was slightly increased by the immobilization technique. Decrease in amperometric response might occur at a higher temperature because of decrement of molecular oxygen in solution or because of thermal deactivation of the enzyme at higher temperatures [35], in this particular case above 40°C.

3.3. Amperometric response of enzyme electrode

Figure 3A illustrates the amperometric (current–time) plot of the constructed biosensor electrode with the presence and absence of Au-NPs. Current response was obtained by successive additions of 10 μM xanthine at an applied potential of 0.70 V in 10 mM PBS (pH 7.0). Both biosensitive electrodes (Chi-PPy/Au-XO and Chi-PPy-XO) showed amperometric responses to injection of xanthine, however the biosensor constructed with Au-NPs exhibited almost five times the higher current response at the point of plateau. The time elapsed to reach the steady state for the Chi-PPy/Au-XO biosensor was two times higher when compared with the Chi-PPy-XO biosensor. The calibration curves of the Chi-PPy/Au-XO and Chi-PPy-XO electrodes are shown in Figure 3B. It was observed that current responses for both biosensors linearly increased with increasing concentrations of xanthine and then reached a plateau. Since xanthine concentration in first 10–15 days is usually smaller than 10 μM, we decided to check biosensor performance using smaller xanthine concentrations. The inset of Figure 3A illustrates the amperometric graph and calibration curve of 1 μM xanthine additions to the Chi-PPy/Au-XO electrode; it can be clearly seen that 10 μM of xanthine addition is equal to 10 × 1 μM additions. We performed the same experiments with Chi-PPy-XO and the results were negative. The linear range was extended from 1 μM to 200 μM in the presence of Au-NPs. The correlation coefficients exhibited good linearity, 0.99364 and 0.99958, from analysis of the responses (inset of Figure 3B). Using a same sample volume of 1 μM and 10 μM, the linear range of the electrode having and lacking Au-NPs was found

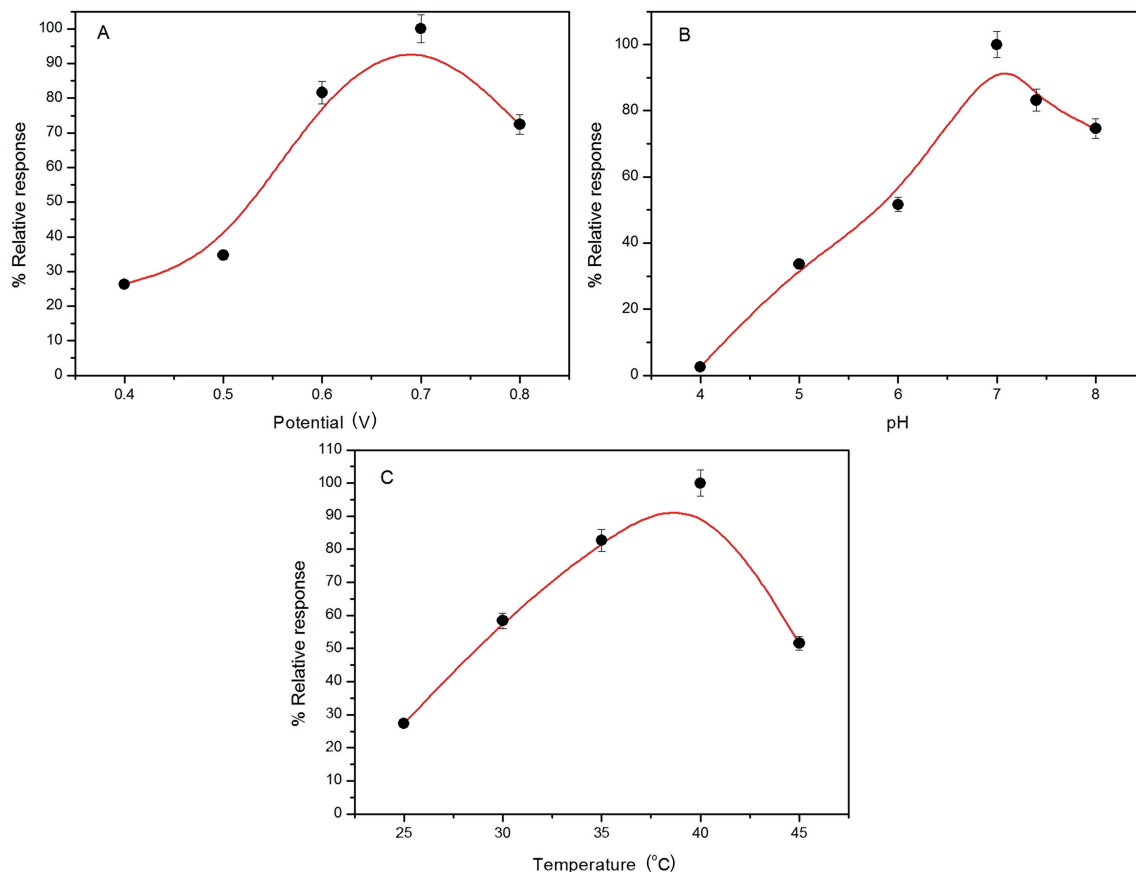


Figure 2 – (A) Effect of applied potential on the response of the biosensing electrode to xanthine substrate (10 mM PBS at pH 7.0). (B) The effect of buffer pH on the response of the biosensing electrode to xanthine (10 mM PBS, + 0.70 V applied potential). (C) The effect of temperature on the amperometric response of the biosensing electrode (10 mM PBS pH 7.0, + 0.70 V applied potential) to substrate addition.

to be from 1 μM to 200 μM and from 10 μM to 90 μM , respectively (inset of Figure 3B) for the amperometric response of biosensors. The sensitivity of the constructed Chi-PPy/Au-XO and Chi-PPy-XO biosensors were also calculated as

1.4 nA/ μM and 0.6 nA/ μM , respectively. The detection limit of the Chi-PPy/Au-XO fabricated electrode is 0.25 μM , which was determined by Eq. (3). These results indicating that current responses obtained from the amperometric

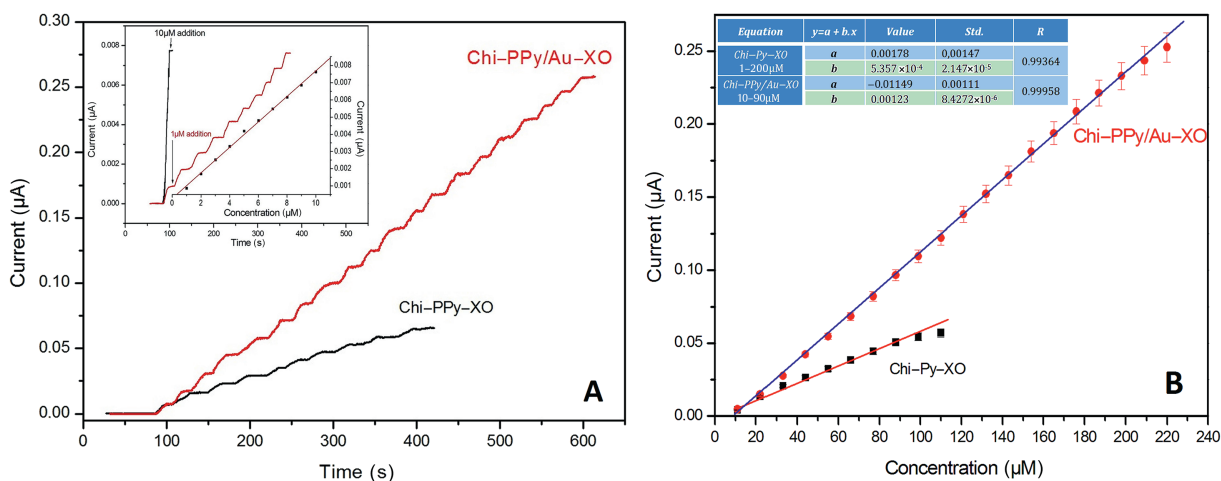


Figure 3 – (A) Amperometric response of biosensing electrodes to successive addition of 10 μM xanthine at an applied potential + 0.70 V in stirred 10 mM PBS (pH 7.0) (Inset: amperometric response of the biosensor to successive addition of 1 μM xanthine). (B) Calibration curves for the amperometric response of the biosensing electrodes.

measurements are both valid, yet electrodes with Au-NPs showed better performance which could be attributed to excellent conductivity, electron transfer ability, and compatible interactions of Au with Chi-PPy.

In order to express viability of the Chi-PPy/Au-XO biosensor, the analytical performance was compared with some of the previously reported xanthine biosensors in Table 1, which indicated that the current biosensor has the wider linear range compared to all other reported works. Most of the work reported is missing important points such as wide linear range, with some work reporting linear range in nanomolar and detection limit picomolar, or reporting wide linear range and detection limit, and therefore missing the measuring xanthine concentration for the first 20 days. The detection limit obtained is very close to the XO/Co3O4/MWCNT/CS/GCE biosensor being quite satisfactory when compared to the other studies. The sensitivity was calculated as 1.4 nA/ μ M and the response time of 8 seconds is an acceptable parameter of the biosensor and wide linear range of 1–200 μ M.

3.4. Operational and storage stability

The reusability of the biosensor was an asset of using the Chi-PPy/Au-NPs/XO electrode, measuring the current response of the electrode by 20 repeated measurements (Figure 4A). All measurements were performed in 10 mM PBS at +0.70 V applied potential, and after each measurement the electrode was stored for recovery at 4°C for 5 minutes. Amperometric response was relatively close for the first five measurements, after which the response starts to gradually decrease and eventually, after 20 repeated measurements, the electrode retained almost 78% of its initial response.

The long-term stability of the Chi-PPy/Au-NPs/XO electrode towards xanthine was assessed by regular experiments over 18 days. To check the long-term storage stability, the electrode was kept in 10 mM PBS, pH 7.0 at 4°C. As shown in Figure 4B, the catalytic current response of xanthine was observed to be lost for 8% in the first 13 days of its initial value, which is most probably due to the xanthine immobilization

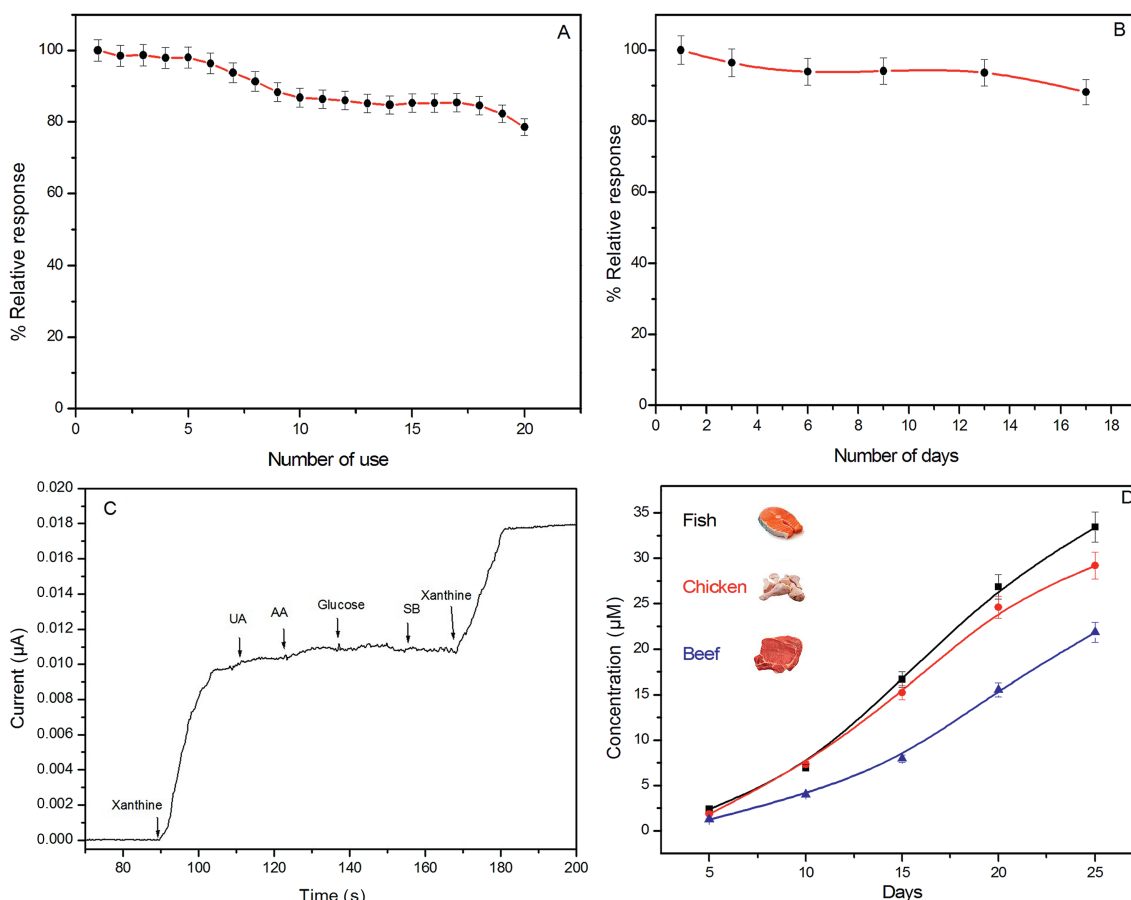


Figure 4 – (A) Operational stability of the biosensing electrode to xanthine additions (10 mM PBS pH 7.0). (B) Long-time stability of biosensing electrode by tracking the amperometric responses of enzyme electrodes in intervals of 18 days (10 mM PBS pH 7.0). (C) Interference effect of potential interferants (uric acid, ascorbic acid, glucose, and sodium benzoate) to the amperometric response of the biosensing electrode (10 mM PBS pH 7.0). (D) Determination of xanthine concentrations in fish, chicken, and beef samples during 25 days (10 mM PBS pH 7.0). AA = ascorbic acid; SB = sodium benzoate; UA = uric acid.

method and biological compatibility of polymer film. Later on, the current response decreased up to ~15% in the 3rd week of long-term storage stability experiments. The reduction in electrocatalytic activity as a function of time of the proposed Chi-PPy/Au-NPs/XO electrode may be caused by denaturation or leakage from the inner membrane solution of XO. In conclusion, the biosensor retained 85% of its initial activity at the end of 18 days of storage.

3.5. Interference, recovery, and real-sample measurements

Analytical recovery experiments of the Chi-PPy/Au-NPs/XO electrode were performed by recording amperometric current responses to known xanthine concentrations, as shown in Table 2 (10 mM, pH 7.0 PBS). As can be clearly seen from amperometric response, the fabricated electrode showed excellent performance in detection of xanthine and very good reliability. The effectiveness of the biosensing electrode has been determined and represented as recovery in the range of 97.4–103.67% with RSD (Relative Standard Deviation) values in the range of 2.45–3.73%, indicating very good reproducibility and reliability of the proposed electrode.

The xanthine amount was calculated using the calibration curve shown in Figure 3B. The effectiveness of the biosensor was calculated by obtaining error rates, from which the high reliability of the proposed method can be observed.

Potential interferant effect on the amperometric current response of the Chi-PPy/Au-NPs/XO electrode was investigated using four different interfering substances: UA, ascorbic acid (AA), glucose, and sodium benzoate (SB) which is widely used in preservation of meat and meat products [36,37] and already used in our previous studies [38,39] (Figure 4C). The interference study showed that there is no remarkable effect on biosensor response caused by interfering substances which are physiologically proportional to a normal level of 10 μM xanthine, 1:1 ratio [40]. It can be observed that the biosensor has small changes when interferants are added. In comparison to selectivity of the biosensor towards xanthine, the amperometric response to interferants is negligible, which resembles the results reported in the literature [41,42]; negligible interference of AA at 0.70 V applied potential was reported for the XO/Au-NPs/GCPE biosensor. The interference study reported by Dalkiran et al [33] should also be noted, where there was negligible interference of glucose, AA, and UA with applied potential of 0.7 V for the amperometric xanthine biosensor based on chitosan- $\text{Co}_3\text{-O}_4$ -multiwall carbon nanotubes.

Table 2 – Analytical performance of Chitosan/PPy/Au-NPs Xanthine biosensor ($n = 3$).

Xanthine added (μM)	Xanthine found (μM)	RSD (%)	Recovery %
1	0.98	2.45	98.0
10	9.75	3.1	97.5
100	103.67	3.73	103.67
200	194.8	2.88	97.4
RSD = .			

Meat quality is a critical issue for the meat industry in the 21st century and has always been important for the customer [43]. Meat has previously been considered essential for human growth and development because it is a concentrated nutrient source [44,45], which gives reason for developing technologies for control, monitoring, and identification of meat quality. Real application of the xanthine biosensor was investigated by measuring xanthine concentrations in fish, chicken, and beef over a period of 25 days of storage. The results of xanthine concentration measurements were interpreted using previously obtained optimum parameters. Detection limit (0.25 μM) and linear range (1–200 μM) of the biosensor were taken into consideration while performing real-sample measurements. As demonstrated in Figure 4D, xanthine concentration drastically increased in the 3rd week and 4th week of storage. The recorded concentration in fish and chicken is almost similar, while beef concentration is much lower in the last 2 weeks. This might be attributed to the fact that beef aging time is longer [46] in comparison to chicken and fish. Real sampling results match those reported by Devi et al [8], as well as concentration values for common fish fillets reported by Balladin et al [47] (1.54–24.7 μM). It is important to indicate that there was no significant change in fish, chicken, or beef meat color, making it difficult to visually differentiate 0-day old beef from 20-day beef. However, measuring the xanthine concentration of given samples demonstrates the extremely bad quality of meat after 25 days, which raises alarm for the development of control, detection, and identification methods of meat aging in meat industries.

4. Conclusion

Results shown in this study exhibited the fabrication (Chi-PPy/Au-XO and Chi-PPy-XO) and application of the bio-nanocomposite film in an amperometric biosensor. In the construction of the biosensor, chitosan, PPy, and Au-NPs were used to build a polymeric matrix by the *in situ* chemical synthesis method on GCE. There is no work reported known to the authors that the xanthine biosensor is designed on, only the simple and straightforward *in situ* chemical synthesis method as described. The use of self-assembled Au-NPs resulted in an improved analytical performance of the biosensor in terms of low response time (~8 seconds), good sensitivity of 1.4 nA/ μM , broader linear range (1–200 μM), and low detection limit of 0.25 μM . Interference study was performed by using possible interfering substances selected as UA, AA, glucose, and SB to verify the selectivity of the sensor, which persisted in the satisfactory range. Real-sample applications were investigated by measuring xanthine concentrations in fish, chicken, and beef in a period of 25 days of storage. Although no visual change was observed in the meat condition, xanthine concentration was recorded in an increasing trend during the 25 days. As a result, the proposed biosensor shows excellent results in xanthine determination and therefore is a very reliable analytical tool for analyzing meat quality; it is also proof for the successful application of hybrid bio-nanocomposite platform in xanthine detection.

Conflicts of interest

The authors declare no conflicts of interest.

Appendix A. Supplementary data

Supplementary data related to this article can be found at <http://dx.doi.org/10.1016/j.jfda.2016.12.005>.

REFERENCES

- [1] Lawal AT, Adeloju SB. Progress and recent advances in fabrication and utilization of hypoxanthine biosensors for meat and fish quality assessment: a review. *Talanta* 2012;100:217–28.
- [2] Kim KY, Schumacher RH, Hunsche E, Wertheimer AI, Kong SX. A literature review of the epidemiology and treatment of acute gout. *Clin Ther* 2003;25:1593–617.
- [3] Kawachi M, Kono N, Mineo I, Yamada Y, Tarui S. Decreased xanthine oxidase activities and increased urinary oxypurines in heterozygotes for hereditary xanthiuria. *Clin Chim Acta* 1990;188:137–46.
- [4] Campion EW, Glynn RJ, Delabry LO. Asymptomatic hyperuricemia. Risks and consequences in the Normative Aging Study. *Am J Med* 1987;82:421–6.
- [5] McMaster-Fay RA. Pre-eclampsia: a disease of oxidative stress resulting from the catabolism of DNA (primarily fetal) to uric acid by xanthine oxidase in the maternal liver; a hypothesis. *Biosci Hypotheses* 2008;1:35–43.
- [6] Chu YH, Chen CJ, Wu SH, Hsieh JF. Inhibition of xanthine oxidase by *Rhodiola crenulate* extracts and their phytochemicals. *J Agric Food Chem* 2014;62:3742–9.
- [7] Shah L. Amperometric determination of fish freshness by a hypoxanthine biosensor. *J Sci Food Agric* 1996;70:298–302.
- [8] Devi R, Batra B, Lata L, Yadav S, Pundir CS. A method for determination of xanthine in meat by amperometric biosensor based on silver nanoparticles/cystein modified Au electrode. *Process Biochem* 2013;48:242–9.
- [9] Renata S, Pagliarussi L, Luis AP, Freitas L, Bastos JK. A quantitative method for the analysis of xanthine alkaloids in *Paullinia cupana* (guarana) by capillary column gas chromatography. *J Sep Sci* 2002;25:371–4.
- [10] Berti G, Fossati P, Tarengi G, Musitelli C, Melzideril GV. Enzymatic colorimetric method for the determination of inorganic phosphorus in serum and urine. *J Clin Chem Clin Biochem* 1988;26:399–404.
- [11] Kock R, Delvoux B, Gresiling H. A high performance liquid chromatographic method for the determination of hypoxanthine, xanthine, uric acid, and allantoin in serum. *J Clin Chem Clin Biochem* 1993;31:303–10.
- [12] Olojoa RQ, Xiab RH, Abramsona JJ. Spectrophotometric and fluorometric assay of superoxide ion using 4-chloro-7-nitrobenzo-2-ox a-1,3-diazole. *Anal Biochem* 2005;339:338–44.
- [13] Yoon Y, Jang J. Conducting-polymer nanomaterials for high-performance sensor applications: issues and challenges. *Adv Funct Mater* 2009;19:1567–76.
- [14] Singh S, Chaubey A, Malhotra BD. Amperometric cholesterol biosensor based on immobilized cholesterol esterase and cholesterol oxidase on conducting polypyrrole films. *Anal Chim Acta* 2004;502:229–34.
- [15] Tuncagil S, Odaci D, Varis S, Timur S, Toppare L. Electrochemical polymerization of 1-(4-nitrophenyl)-2,5-di(2-thienyl)-1 H-pyrrole as a novel immobilization platform for microbial sensing. *Bioelectrochemistry* 2009;76:169–74.
- [16] Philippova OE, Volkov EV, Sitnikova ML, Khokhlov AR, Desbrieres J, Rinaudo M. Two types of hydrophobic aggregates in aqueous solutions of chitosan and its hydrophobic derivative. *Biomacromolecules* 2001;2:483–90.
- [17] Susanto H, Samsudin AM, Rokhati N, Widiasa IN. Immobilization of glucose oxidase on chitosan-based porous composite membranes and their potential use in biosensors. *Enzyme Microb Technol* 2013;52:386–92.
- [18] Mokhodoeva OB, Myasoedova GV, Kubrakova IV. Sorption preconcentration in combined methods for the determination of noble metals. *Anal Chem* 2007;62:607–22.
- [19] Mikoliūnaitė L, Kubiliūtė R, Popov A, Voronovič J, Šakirzanovas S, Ramanavičienė A, Ramanavičius A. Development of gold nanoparticle-polypyrrole nanocomposites. *Chemija* 2014;25:63–9.
- [20] Segawa H, Shimidzu T, Honda K. A novel photo-sensitized polymerization of pyrrole. *Chem Soc Chem Commun* 1989;2:132–3.
- [21] Senel M, Nergiz C. Novel amperometric glucose biosensor based on covalent immobilization of glucose oxidase on poly(pyrrole propylic acid)/Au nanocomposite. *Curr Appl Phys* 2012;12:1118–24.
- [22] Qiu JD, Liang RP, Wang R, Fan LX, Chen YW, Xia XH. A label-free amperometric immunosensor based on biocompatible conductive redox chitosan-ferrocene/gold nanoparticles matrix. *Biosens Bioelectron* 2009;25:852–7.
- [23] Sarathy KV, Narayan KS, Kim J, White JO. Novel fluorescence and morphological structures in gold nanoparticle-polyoctylthiophene based thin films. *Chem Phys Lett* 2000;318:543–8.
- [24] Rosi N, Mirkin C. Nanostructures in biodiagnostics. *Chem Rev* 2005;105:1547–62.
- [25] Santos DS, Goulet PJG, Pieczonka NPW, Oliveira ON, Aroca NF. Gold nanoparticle embedded, self-sustained chitosan films as substrates for surface-enhanced raman scattering. *Langmuir* 2004;20:10273–7.
- [26] Njagi J, Andreescu S. Stable enzyme biosensors based on chemically synthesized Au–polypyrrole nanocomposites. *Biosens Bioelectron* 2007;23:168–75.
- [27] Wolowacz SE, Yon-Hin BFY, Lowe CR. Covalent electropolymerization of glucose oxidase in polypyrrole. *Anal Chem* 1992;64:1541–5.
- [28] Liu CG, Desai KG, Chen XG, Park HJ. Linolenic acid-modified chitosan for formation of self-assembled nanoparticles. *Agric Food Chem* 2005;53:437–41.
- [29] Borgmann S, Schulte A, Neugebauer S, Schuhmann W. Amperometric biosensors. In: Richard CA, Dieter MK, Jacek L, editors. *Advances in electrochemical science and engineering: Bioelectrochemistry*; 2012. p. 1–83.
- [30] Burke LD, Nugent PF. The electrochemistry of gold: I the redox behaviour of the metal in aqueous media. *Gold Bull* 1997;30:43–53.
- [31] Zheng B, Xie S, Qian L, Yuan H, Xiao D, Choi MMF. Gold nanoparticles-coated eggshell membrane with immobilized glucose oxidase for fabrication of glucose biosensor. *Sens Actuators B Chem* 2011;152:49–55.
- [32] Lin J, He C, Zhang L, Zhang S. Sensitive amperometric immunosensor for alpha-fetoprotein based on carbon nanotube/gold nanoparticle doped chitosan film. *Anal Biochem* 2009;384:130–5.
- [33] Dalkiran B, Kaçar C, Erden PE, Kilic E. Amperometric xanthine biosensors based on chitosan-Co3O4-multiwall carbon nanotube modified glassy carbon electrode. *Sens Actuators B Chem* 2014;200:83–91.
- [34] Devi R, Thakur M, Pundir CS. Construction and application of an amper-ometric xanthine biosensor based on zinc oxide

- nanoparticles-polypyrrole composite film. *Biosens Bioelectron* 2011;26:3420–6.
- [35] Pei J, Li XY. Xanthine and hypoxanthine sensors based on xanthine oxidase immobilized on a CuPtCl₆ chemically modified electrode and liquid chromatography electrochemical detection. *Anal Chim Acta* 2000;414:205–13.
- [36] Ruiz-Capillas C, Jimenez-Colmenero F. Determination of preservatives in meat products by flow injection analysis (FIA). *Food Addit Contam Part A Chem Anal Control Expo Risk Assess* 2008;25:1167–78.
- [37] Clarke EGC, Humphreys DJ, Stoilis E. Determination of benzoic acid in meat and meat products by gas chromatography. *Analyst* 1972;97:433–6.
- [38] Dervisevic M, Dervisevic E, Azak H, Cevik E, Senel M, Yildiz HB. Novel amperometric xanthine biosensor based on xanthine oxidase immobilized on electrochemically polymerized 10-[4H-dithieno(3,2-b:2,3-d)pyrrole-4-yl]decane-1-amine film. *Sens Actuators B Chem* 2016;225:181–7.
- [39] Dervisevic M, Custiuc E, Cevik E, Senel M. Construction of novel xanthine biosensor by using polymeric mediator/MWCNT nanocomposite layer for fish freshness detection. *Food Chem* 2015;181:277–83.
- [40] Cass AEG, Davis G, Francis DG, Hill HAO, Aston WJ, Higgins LJ, Plotkin EV, Scott LDL, Turner APF. Ferrocene-mediated enzyme electrode for amperometric determination of glucose. *Anal Chem* 1984;56:667–71.
- [41] Xu F, Wang L, Gao M, Jin L, Jin J. Amperometric sensor for glucose and hypoxanthine based on a PdIrO₂ modified electrode by a co-crosslinking bienzymic system. *Talanta* 2002;57:365–73.
- [42] Çubukçu M, Timur S, Anik U. Examination of performance of glassy carbon paste electrode modified with gold nanoparticle and xanthine oxidase for xanthine and hypoxanthine detection. *Talanta* 2007;74:434–9.
- [43] Joo ST, Kim GD, Hwang YH, Ryu YC. Control of fresh meat quality through manipulation of muscle fiber characteristics. *Meat Sci* 2013;95:828–36.
- [44] Pereira PMCC, Vicente AFRB. Meat nutritional composition and nutritive role in the human diet. *Meat Sci* 2013;93:586–92.
- [45] Higgs JD. The changing nature of red meat: 20 years of improving nutritional quality. *Trends Food Sci Tech* 2000;11:85–95.
- [46] Yano Y, Kafaho N, Watanabe M, Nakamura T, Asano Y. Evaluation of beef aging by determination of hypoxanthine and hypoxanthine contents; application of xanthine sensor. *Food Chem* 1995;52:439–45.
- [47] Balladin D, Narinesingh D, Stoute V, Ngo T. Immobilization of xanthine oxidase and its use in the quantitation of hypoxanthine in fish muscle tissue extracts using a flow injection method. *Appl Biochem Biotechnol* 1997;62:317–28.
- [48] Lawal AT, Adeloju SB. Comparison of polypyrrole-based xanthine oxidase amperometric and potentiometric biosensors for hypoxanthine. *J Mol Catal B Enzym* 2010;66:270–5.
- [49] Kirgöz ÜA, Timur S, Wang J, Telefoncu A. Xanthine oxidase modified glassy carbon paste electrode. *Electrochem Commun* 2004;6:913–6.
- [50] Pundir CS, Devi R, Narang J, Singh S, Shewta J. Fabrication of an amperometric xanthine biosensor based on polyvinylchloride membrane. *Food Biochem* 2012;36:21–7.
- [51] Villalonga R, Camacho C, Cao R, Hernandez J, Matías JC. Amperometric biosensor for xanthine with supramolecular architecture. *Chem Commun* 2007;9:942–4.
- [52] Dervisevic M, Custiuc E, Cevik E, Durmus Z, Senel M, Durmus A. Electrochemical biosensor based on REGO/Fe₃O₄ bionanocomposite interface for xanthine detection in fish sample. *Food Cont* 2015;57:402–10.
- [53] Lawal AT, Adeloju SB. Mediated xanthine oxidase potentiometric biosensors for hypoxanthine based on ferrocene carboxylic acid modified electrode. *Food Chem* 2012;135:2982–7.
- [54] Thandavan K, Gandhi S, Sethuraman S, Rayappan JBB, Krishna UM. Development of electrochemical biosensor with nano-interface for xanthine sensing – A novel approach for fish freshness estimation. *Food Chem* 2013;139:963–9.
- [55] Devi R, Yadav S, Pundir CS. Electrochemical detection of xanthine in fish meat by xanthine oxidase immobilized on carboxylated multiwalled carbon nanotubes/polyaniline composite film. *Biochem Eng* 2011;58:148–53.
- [56] Dimcheva N, Horozova E, Jordanova Z. An Amperometric xanthine oxidase enzyme electrode based on hydrogen peroxide electro-reduction. *J Biosci* 2002;57:883–9.